IOPscience iopscience.iop.org

Home Search Collections Journals About Contact us My IOPscience

The low energy excess of vibrational states in v-SiO_2: the role of transverse dynamics

This article has been downloaded from IOPscience. Please scroll down to see the full text article.

2004 J. Phys.: Condens. Matter 16 8519

(http://iopscience.iop.org/0953-8984/16/47/006)

View the table of contents for this issue, or go to the journal homepage for more

Download details:
IP Address: 129.252.86.83
The article was downloaded on 27/05/2010 at 19:09

Please note that terms and conditions apply.

INSTITUTE OF PHYSICS PUBLISHING JOURNAL OF PHYSICS: CONDENSED MATTER

J. Phys.: Condens. Matter **16** (2004) 8519–8530 PII: S0953-8984(04)83794-9

The low energy excess of vibrational states in v-SiO_2: the role of transverse dynamics

O Pilla[1,7], S Caponi[1,2], A Fontana[1,2], J R Gonçalves[1,3], M Montagna[1], F Rossi[1], G Viliani[1,2,8], L Angelani[4,5], G Ruocco[2,4], G Monaco[6] and F Sette[6]

[1] Dipartimento di Fisica, Università di Trento, 38050 Povo, Trento, Italy
[2] INFM-CRS SOFT, Università di Roma La Sapienza, 00185 Roma, Italy
[3] Departmento de Física, Universidade do Ceará, 60455-760 Fortaleza, Ceará, Brazil
[4] Dipartimento di Fisica, Università di Roma La Sapienza, 00185 Roma, Italy
[5] INFM-CRS SMC, Università di Roma La Sapienza, 00185 Roma, Italy
[6] European Synchrotron Radiation Facility, BP 220, 38043 Grenoble, France

E-mail: viliani@science.unitn.it

Received 19 July 2004
Published 12 November 2004
Online at stacks.iop.org/JPhysCM/16/8519
doi:10.1088/0953-8984/16/47/006

Abstract

A numerical simulation study of the density dependence ($\rho = 2.2$–4.0 g cm^{-3}) of the high energy collective dynamics in vitreous silica at mesoscopic wavevectors ($Q = 1$–18 nm^{-1}) is reported. The dynamic structure factor, $S(Q, \omega)$, and the density of states, $\rho(E)$, have been determined in the harmonic approximation via the system eigenvalues and the eigenvectors, in turn obtained by the direct diagonalization of the dynamical matrix. The BKS interaction potential employed is capable of reproducing the experimentally observed excess of states (boson peak), and its density dependence. The numerical simulation also indicates a strong density dependence of the transverse excitation dispersion relation, $\Omega_T(Q)$, at large Q. Specifically, $\Omega_T(Q)$ is found to flatten at high Q to a value that increases with increasing density. The parallel between the density dependent flattening of $\Omega_T(Q)$ and the density dependence of the boson peak suggests that the latter feature arises from the high Q portion of the transverse branch. This hypothesis is in line with both the interpretation by Elliott and co-workers (Taraskin *et al* 2001 *Phys. Rev. Lett.* **86** 1255), who assign the boson peak to a phenomenon in glass reminiscent of the lowest energy Van Hove singularity in the companion crystal, and the Buchenau *et al* (1986 *Phys. Rev.* B **34** 5665) assignment of the boson peak to the localized hindered rotation of SiO_2 tetrahedra.

[7] Deceased.
[8] Author to whom any correspondence should be addressed.

 © 2004 IOP Publishing Ltd Printed in the UK

1. Introduction

Insulating disordered solids, when compared to their crystalline counterparts, exhibit some common peculiarities in their low temperature thermal properties and low energy spectroscopic features [1, 2], in particular: (i) a larger specific heat at temperatures up to ≈1 K, ascribed to tunnelling processes [3, 4]; (ii) a much smaller thermal conductivity, which also shows a plateau in the temperature range ≈1–10 K [1]; (iii) a quasi-elastic light scattering and neutron scattering intensity; and, most important, (iv) an excess of modes in the vibrational density of states, known as the boson peak (BP). An unambiguous understanding of the origin of these extra modes, and of their possible relation with other reported anomalies, is still lacking, in spite of the extensive research effort primed by the pioneering work of Buchenau *et al* [5] and continued by many authors [6–14]. No definite conclusion has yet been drawn as to the nature of the vibrational eigenvectors of the modes responsible for the BP. In fact, according to different authors, they are either spatially localized [5, 7], spatially delocalized and propagating [6, 9, 13], or spatially delocalized but diffusive in character [15]. Even more important, we still do not completely understand why disorder should accumulate vibrational eigenvalues in the same energy region, in such a broad variety of chemically and physically different materials. Some recent theoretical works have been devoted to this subject, and among them we recall:

(i) the work of Elliott and co-workers, who assigned the BP in glasses to the lowest energy van Hove singularity of the corresponding crystal [14, 16, 17];
(ii) the work of Grigera *et al*, who interpreted the BP as the precursor of the dynamical instability expected in a disordered structure as a function of density [18]; and
(iii) the work of Götze and Mayr [19] and that of Schilling *et al* [20], who obtained a spectral feature recalling the BP within a mode-coupling-like description of the high frequency dynamics of a model glass.

In the specific case of v-SiO_2 at normal density, the most widely accepted explanation is that the BP originates from the piling up of modes near the first van Hove singularity of the transverse acoustic vibrational branch [14, 16]. These modes should mainly involve relative rotations of almost rigid SiO_4 tetrahedra, as pointed out early on by Buchenau and co-workers [5]. In addition to the ambient pressure data, useful information is available for v-SiO_2 at higher densities, obtained both from *in situ* measurements on samples under pressure and from permanently densified samples. In general, densification results in a shift of the BP towards higher energies and in a simultaneous decrease of its intensity [21–24]. In addition to the experimental data, the behaviour of the BP with density has been successfully reproduced by a series of simulations [25–27]. Recently, very accurate inelastic neutron scattering (INS) measurements on densified vitreous silica (d-SiO_2) have confirmed these effects [28–30]. In densified samples, the BP lies at higher energies with respect to normal density, and its intensity is lower. Moreover, in densified samples the inelastic signal in the BP energy range shows a more marked dependence on the scattering wavevector Q, as regards its intensity and peak position.

We present here simulation results on v-SiO_2 at different densities which, when compared with the existing experimental data, can help in clarifying the origin and the nature of the excess modes, as well as the intensity and shift effects on the BP as a function of density. Specifically, we find a *qualitative* change in the shape of the transverse acoustic branch when the density is changed: while at the lowest (ambient) density it shows a linear dispersion for $Q < 8$ nm^{-1} ($\Omega_T(Q) \approx v_T Q$) and a flattening above this value at $\hbar\Omega(Q) \approx 20$ meV, at the highest density studied the dispersion relation becomes linear over the whole Q range, reaching values as high

as 60 meV. By comparing this behaviour with the experimental observation that, on increasing the density, in vitreous silica the BP undergoes a blue-shift and becomes less and less intense, we suggest that the extra modes which pile up in the BP region have a transverse acoustic nature. Our results quantitatively support (i) Elliott and co-workers' proposal [14, 17] that the BP is connected to the lowest van Hove singularity of crystalline quartz, and (ii) the Buchenau *et al* finding [5] that the modes at the BP are local rotations of SiO_4 tetrahedra.

2. Simulation details

The systems investigated consist of 680 SiO_2 units ($N = 2040$ ions), enclosed in cubic boxes of different lengths (from $L = 3.1359$ nm, corresponding to $\rho = 2.2$ g cm^{-3} for the glass at room pressure, down to $L = 2.5693$ nm corresponding to a density of 4.0 g cm^{-3}), with periodic boundary conditions. The ions interact through the BKS [31] two-body potential; the long range interaction was treated by the Ewald sum technique. As has already been demonstrated, this potential reproduces quantitatively the high frequency dynamics of vitreous silica [32]. The glass configuration at room pressure was obtained by standard MD methods for lowering the temperature down to 300 K, starting from a well equilibrated liquid configuration at $T = 6000$ K; a conjugate gradient geometrical minimization on the potential energy hypersurface was subsequently performed, for an accurate location of the minimum. Such a minimum configuration was in turn taken as the starting point for generating a series of compressed systems. At each compression step, the box size was scaled by $\approx$1.5% and the system was allowed to relax, after which the new minimum configuration was searched for by the conjugate gradient method. This procedure was repeated until the final density of 4.0 g cm^{-3} (corresponding to a sample under a hydrostatic pressure of about 35 GPa [21]) was reached. A complete study of the structural and dynamical changes occurring during the compression will be presented elsewhere. We focus here on the changes in the *high frequency dynamics* that take place as the density is increased.

The vibrational dynamics in the minimum configurations was computed in the harmonic approximation by diagonalizing the dynamical matrix, to obtain the eigenvalues (ω_p) and eigenvectors ($e_p(i)$) of the pth normal mode ($p = 1$–$3N$). From these quantities all vibrational characteristics can be derived. In particular, we have computed the dynamic structure factor $S(Q, \omega)$ as well as the longitudinal (L) and transverse (T) current spectra ($C^\eta(Q, \omega)$) which, in the one-excitation approximation, are given by

$$\begin{aligned} S_{\alpha\beta}(Q,\omega) &= \frac{K_B T Q^2}{\sqrt{M_\alpha M_\beta}} \sum_p E_p^{\mathrm{L}}(\alpha,\beta;Q)\frac{1}{\omega_p^2}\delta(\omega-\omega_p) \\ C_{\alpha\beta}^{\eta}(Q,\omega) &= \frac{K_B T}{\sqrt{M_\alpha M_\beta}} \sum_p E_p^{\eta}(\alpha,\beta;Q)\delta(\omega-\omega_p) \end{aligned} \tag{1}$$

where $\eta \in \{\mathrm{L}, \mathrm{T}\}$, α, β indicate Si and O, and $E_p^\eta(Q)$ is the spatial power spectrum of the (longitudinal or transverse) component of the eigenvectors:

$$\begin{aligned} E_p^{\mathrm{L}}(\alpha,\beta;Q) &= \frac{1}{\sqrt{N_\alpha N_\beta}} \sum_{i\in\alpha}^{N_\alpha}\sum_{j\in\beta}^{N_\beta} [\hat{Q}\cdot\bar{e}_p(i)][\hat{Q}\cdot\bar{e}_p(j)]\mathrm{e}^{\mathrm{i}\bar{Q}\cdot(\bar{R}_i-\bar{R}_j)} \\ E_p^{\mathrm{T}}(\alpha,\beta;Q) &= \frac{1}{\sqrt{N_\alpha N_\beta}} \sum_{i\in\alpha}^{N_\alpha}\sum_{j\in\beta}^{N_\beta} [\hat{Q}\cdot\bar{e}_p(i)]\times[\hat{Q}\cdot\bar{e}_p(j)]\mathrm{e}^{\mathrm{i}\bar{Q}\cdot(\bar{R}_i-\bar{R}_j)}. \end{aligned} \tag{2}$$

Here $\hat{Q} = \bar{Q}/|Q|$ and R_i is the equilibrium position of the ith particle.

The harmonic and one-excitation approximations, used to calculate the dynamic quantities, have been shown to give good agreement with the experimental spectra [9], indicating that the contribution from anharmonicity or from more elusive local motions (for example, that of the two-level systems whose detailed description is fundamental for the explanation of the low temperature properties) are irrelevant in the frequency region investigated.

Once the partial dynamics structure factors or current spectra have been calculated, we analyse the 'experimental' quantities, i.e. their combinations that appear in a (coherent) neutron scattering experiment:

$$S_{\mathrm{N}}(Q,\omega) = \sum_{\alpha\beta} b_\alpha b_\beta S_{\alpha\beta}(Q,\omega) \Big/ \sum_{\alpha\beta} b_\alpha b_\beta \tag{3}$$

and in an inelastic x-ray scattering experiment:

$$S_{\mathrm{X}}(Q,\omega) = \sum_{\alpha\beta} f_\alpha(Q) f^*_\beta(Q) S_{\alpha\beta}(Q,\omega) \Big/ \sum_{\alpha\beta} f_\alpha(Q) f^*_\beta(Q) \tag{4}$$

where b_α is the (coherent) thermal neutron scattering length for atomic species α and $f_\alpha(Q)$ is its atomic form factor, a quantity that is equal to Z_α (the atomic number) in the $Q \to 0$ limit. It is worth noting that, for the specific case of vitreous silica, as the ratio M_α/Z_α is the same for oxygen and silica, the x-ray weighted dynamics structure factor in the small Q limit coincides with the density–density correlation function. In the following we will present the x-ray weighted dynamics quantity.

3. Discussion

3.1. Current spectra

Usually, the dynamical data obtained via simulation are reported showing the dynamic structure factor, $S(Q,\omega)$, because this procedure has the advantage of being directly comparable to the experimental spectra obtained, for instance, from standard INS and inelastic x-ray scattering (IXS) measurements. On the other hand, the longitudinal current spectra, that turn out to be related to the dynamic structure factor (see equation (1)) via $C^{\mathrm{L}}(Q,\omega) = \omega^2 S(Q,\omega)/Q^2$, are much more useful when one is interested in characterizing the vibrational spectra. In fact, as can be seen from equation (1), each current spectrum taken at a fixed ω directly gives the spatial power spectrum of the eigenvectors at the selected frequency. Thus one can, for example, distinguish between 'plane waves'—characterized by a sharp peak in Q space resulting from Fourier transforming $e_p(i) \approx \exp(\mathrm{i}\bar{k}_p \cdot \bar{R}_i)$—and localized modes, where the fact that $e_p(i)$ is non-zero only for few nearby atoms gives rise to a broad spectrum in Q space. Moreover, in analysing the experimental data, usually one performs the fitting procedure directly on the measured quantity (i.e. the $S(Q,\omega)$), but—on plotting the dispersion relation $\Omega(Q)$—it is the maximum of the current spectra (*and not* of $S(Q,\omega)$) that is reported. In this respect, it is worth recalling that in the celebrated DHO model (the appropriate model for the dynamic structure factor in the memory function approach when the structural relaxation process is frozen [33] as in the case of harmonic glasses)

$$S_{\mathrm{DHO}}(Q,\omega) = \frac{S(Q)}{\pi} \frac{\Omega^2(Q)\Gamma(Q)}{(\omega^2 - \Omega^2(Q))^2 + \Gamma^2(Q)\omega^2} \tag{5}$$

it is the parameter $\Omega(Q)$ that represents the excitation frequency. Straightforward algebra shows that $\Omega(Q)$ is the maximum of $\omega^2 S_{\mathrm{DHO}}(Q,\omega)$ and not of $S_{\mathrm{DHO}}(Q,\omega)$. The difference between $\Omega(Q)$ and the maximum of $S_{\mathrm{DHO}}(Q,\omega)$ (located at $\sqrt{\Omega^2(Q) - \Gamma^2(Q)/2}$) is small

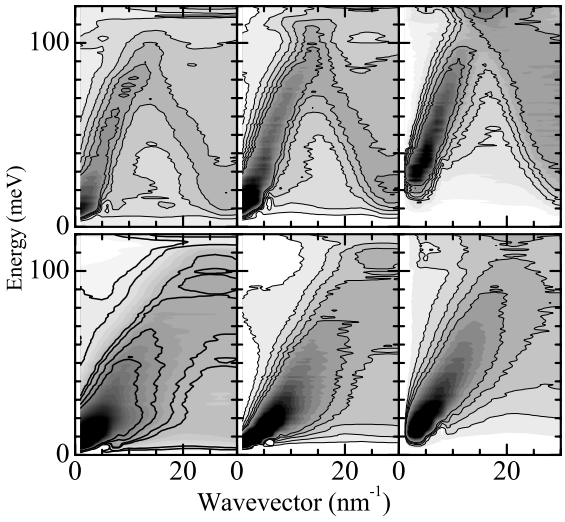

Figure 1. An overview of computed neutron weighted current spectra of v-SiO_2 at three different densities (from left to right): $\rho = 2.2$ g cm^{-3} ($P = 0$ GPa), $\rho = 2.8$ g cm^{-3} ($P = 0$ GPa densified); $\rho = 4.0$ g cm^{-3} ($P = 35$ GPa). Top: longitudinal currents; bottom: transverse currents. The current spectra have been divided by Q^2 for visualization purposes. In the greyscale maps, the black region correspond to high values of the current spectra, the white region corresponds to zero.

for small values of $\Gamma(Q)$, but becomes important in those cases where the high Q (and thus high $\Gamma(Q)$) dynamics is studied.

The computed current spectra, for both longitudinal and transverse dynamics, are shown in figure 1 (upper and lower panel, respectively) as a contour-map plot for v-SiO_2 at $\rho = 2.2, 2.8, 4.0$ g cm^{-3}. The most evident feature is that in the longitudinal currents a periodicity is present, even if much less evident than for a crystal. The same feature is present in the transverse ones, but with a longer quasi-period which extends beyond the limit of the figure.

As discussed by Taraskin and Elliott [16] and in [27] this difference is due to the fact that the longitudinal dynamics is affected by the average height of the SiO_4 tetrahedron, which is the main structural unit of v-SiO_2, while the transverse vibrations are sensitive to the average height of the SiO_4 tetrahedron decorated with oxygen atoms. In the low Q longitudinal spectrum, in addition to the quasi-periodic pattern, two readily observable features are present in the two lowest density samples, which consist of protruding peninsulas, nearly parallel to the Q axis, centred at about 20 and 100 meV. These features have been interpreted [16] as a trace of the vibrational dynamics of the cristobalite structure (the crystalline counterpart of v-SiO_2), which shows in that energy range flat dispersion bands. It should be noted that the plots of figure 1 are shown as a function of the modulus of the wavevector, which is a relevant quantity for glasses, thus losing all information on the Q direction. If this convention were also used in representing the dispersion curves of a crystal, different Q directions in the Brillouin zone would superimpose giving qualitatively the same effect as in figure 1. In the Q–E range between 5 and 15 nm^{-1} and 10 to 25 meV (where the flat band is observed in the longitudinal currents), a much more evident flattening is present in the transverse currents. This coincidence has suggested the interpretation that the flattened band in the longitudinal currents arises from a spilling of transverse dynamics into the longitudinal one, due to disorder [16, 27, 34].

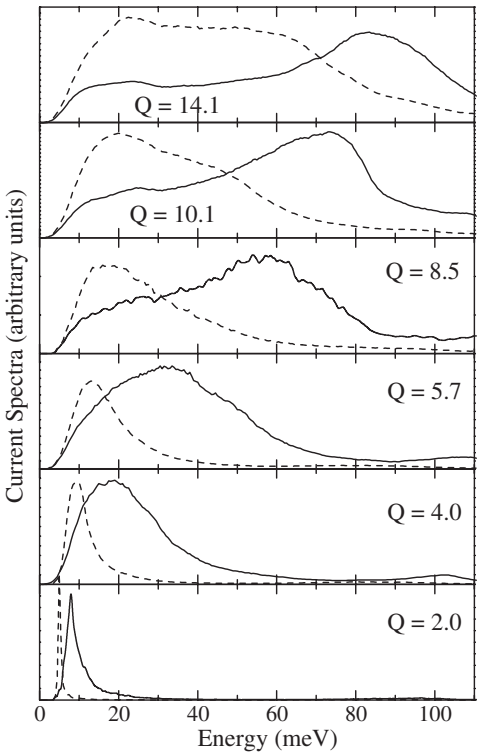

Figure 2. Selected examples of longitudinal (full curves) and transverse (dashed curves) current spectra at the Q values, indicated in nm^{-1}, for the sample at $\rho = 2.2$ g cm^{-3}.

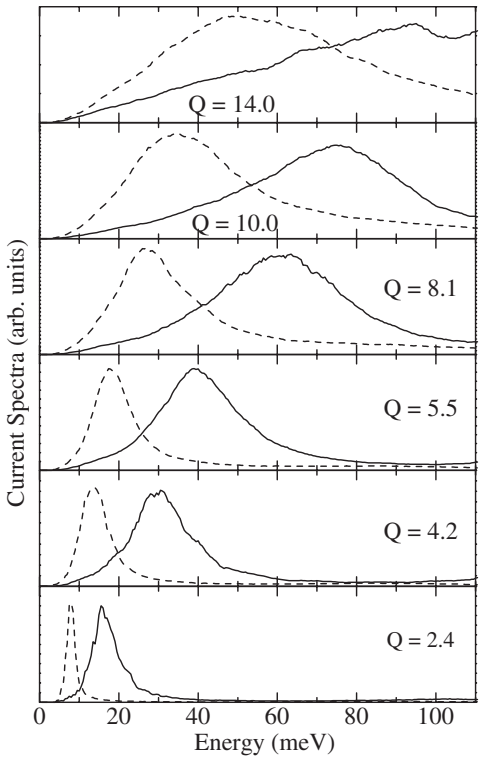

Figure 3. Selected examples of longitudinal (full curves) and transverse (dashed curves) current spectra at the Q values indicated (in nm^{-1}) for the highest density sample ($\rho = 4.0$ g cm^{-3}).

In figure 2 we report longitudinal and transverse current spectra at selected Q values for the uncompressed sample ($\rho = 2.2$ g cm^{-3}). For Q values larger than about 8 nm^{-1}, both $C^{L}(Q, \omega)$ and $C^{T}(Q, \omega)$ show two distinct excitation maxima, and this double-excitation structure becomes more and more evident with increasing Q values. The excitation at higher energy disperses with Q and is observed at all Q values in the longitudinal current spectra, while it shows up as a weak shoulder in the transverse current spectra only at $Q > 10\,nm^{-1}$. In agreement with previous findings [9, 16, 32], we assign this feature to the longitudinal sound-like branch. The behaviour of the low energy excitation is in some sense complementary: it is always present in the transverse current spectra, while it appears in the longitudinal currents only at $Q > 8$ nm^{-1}. At small Q, the low energy peak disperses linearly with a sound velocity of $\approx$3800 m s^{-1} (appropriate for the transverse sound modes), and becomes almost non-dispersing at $Q > 8$ nm^{-1}. We will call this low energy feature—which is the main feature in the transverse current spectra—the transverse acoustic mode.

The presence of the signature of transverse dynamics in the *longitudinal* current spectra, and vice versa, is only apparently surprising. Indeed, the polarization character of the modes (which is better and better defined with increasing wavelength, i.e. when the vibration 'sees' the medium as an elastic continuum) becomes ill defined at short wavelengths. This *mixing* phenomenon has already been observed in the simulated [35] and experimental [36] spectra of liquid water. The mixing phenomenon lies at the basis of the growth of peaks associated

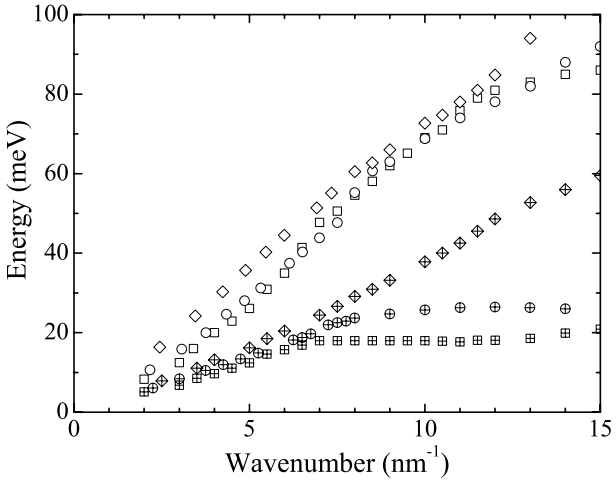

Figure 4. Main maxima of the longitudinal (open symbols) and transverse (crossed symbols) current spectra, for three different densities. Squares: $\rho = 2.2$ g cm^{-3} ($P = 0$ GPa); diamonds: $\rho = 4.0$ g cm^{-3}; circles $\rho = 2.8$ g cm^{-3} ($P = 0$ GPa densified).

with the opposite polarization modes in the current spectra, and of the increased visibility of these peaks with increasing Q values.

Spectra similar to those of figure 2, but for the sample at the highest density studied ($\rho = 4.0$ g cm^{-3}), are reported in figure 3. One can observe that the two current spectra are now 'pure', and no evidence of wrongly polarized modes is present; moreover, and more importantly, the T branch no longer shows a flattening. The maxima of the longitudinal and of the transverse currents in the constant Q cuts are reported in figure 4 for three selected mass densities.

In the starting configuration, $\rho = 2.2$ g cm^{-3}, open and crossed squares of figure 4, the main maxima relative to the longitudinal currents have a well defined dispersing character up to very high energies (about 100 meV), while the transverse dispersion is linear at small Q and at $Q \approx 7$ nm^{-1} flattens at an energy $\approx$20 meV. The main maxima of the transverse current remain centred, within the uncertainty, at the same energy at which the minor peak is observed also in the longitudinal current spectra, whose intensity is roughly 50–80% of the main feature. On increasing the density to 4.0 g cm^{-3}, the local structure of the glass, which at normal density consists of fourfold-coordinated Si ions, is almost completely replaced by an octahedral one (typical of stishovite, i.e. the crystalline form of silica stable at high densities). As a consequence of this local structure transformation, the dynamical properties also change and this can be seen in figure 4. Both longitudinal and transverse maxima follow a nearly linear dispersion law up to the highest reported Q and no flattening of the transverse branch is observed. The important result which emerges from figure 4 is that the 'transverse' branches in low and intermediate density samples, and at large Q values, flatten to an energy value which increases with increasing density ($\approx$15 meV at room conditions, 2.2 g cm^{-3}, and $Q = 10$ nm^{-1}).

The density of vibrational states ($g(E)$), associated with the branches which flatten, will obviously have an excess of modes with respect to the Debye behaviour at these energies, reminiscent of the van Hove singularity of the corresponding crystal [14]: the boson peak.

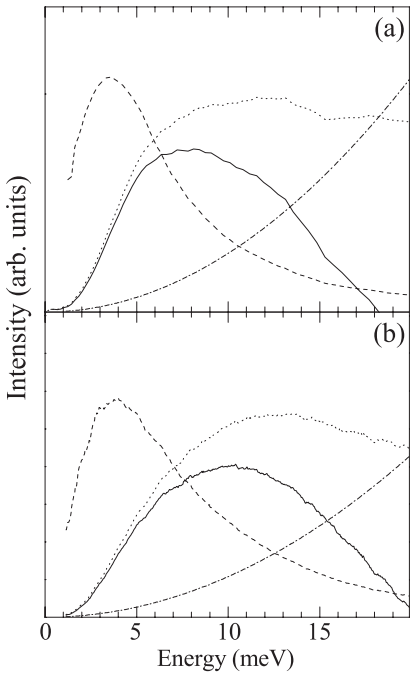

Figure 5. (a) Dotted curve: INS density of states of v-SiO_2; dash–dotted curve: Debye approximation; full curve: vibrational excess, i.e. whole DOS minus Debye DOS; dashed curve: density of states divided by E^2. (b) As (a), but for the unpolarized Raman spectrum of v-SiO_2. Here the full line represents the density of states weighted by the Raman coupling function.

3.2. Boson peak

Experimentally, in v-SiO_2 at room pressure, the excess of modes appears as a broad peak in the plot of the Debye-normalized density of states $g(E)/E^2$. It turns out to be centred at $\approx$5 meV and to have a width of $\approx$5 meV. In order to establish a comparison between the simulation results and the experimental data, it is important to stress that the presence of the $1/E^2$ factor severely affects the appearance of the spectral distribution of the excess of states, by strongly enhancing their low energy tail. Indeed, the true excess of states should be observed in the *difference* between the actual density of states ($g(E)$) and its Debye approximation ($g_D(E)$). Therefore, the experimental determination of the actual shape of the vibrational excess implies knowledge not only of the density of states, but also of the relative weight of the crystalline one, or at least its Debye approximation. The density of states can be obtained from inelastic neutron scattering data, and also, to a certain extent, from depolarized Raman data. The Debye density of states can be independently estimated via Brillouin light scattering, while heat capacity experiments give the appropriate normalization factors [5, 37]. The result of this procedure, using literature data, is shown in figure 5. Here the INS-deduced $g(E)$ is shown together with the Debye contribution obtained via the knowledge of the low frequency (GHz range) L and T sound velocities. The excess of states (the full line in the figure) is obtained by subtracting the Debye DOS from the whole DOS, and the boson peak (i.e. the excess in $g(E)/E^2$) is obtained by dividing the latter quantity by E^2. The most important message arising from figure 5 is that the *true excess of states* is a very broad and featureless band centred at energies much higher than 5 meV, i.e. the 'energy' usually associated with the boson peak. Actually, the observed BP

lies on the low energy tail of the true excess of states, since the contribution of the remaining high energy vibrations is almost suppressed by the $1/E^2$ factor. A similar effect is observed also in the depolarized Raman spectra (lower panel of figure 5). Here one does not observe directly the density of states, but this quantity weighed by the Raman coupling function [38]. A qualitatively similar behaviour is found even if the scattered intensity is somewhat deformed by the Raman coupling function $C(E)$.

Summing up, the conclusion that can be drawn from figures 5 and 4 (concerning the normal density data) is that the excess of density of states accumulates in a broad region, certainly covering the 10–20 meV region, which is almost coincident with the energy region where the transverse branch flattens. Therefore, the analysis of the normal density data leads us to hypothesize that *the BP arises from the high Q portion of the transverse branch*.

The quantitative difference between the position of the flattening of the transverse branch as found in simulations (about 20 meV as in figure 4) and the maximum of the excess of states derived experimentally (the broad band extending from 10 to 20 meV as in figure 5), can derive from different causes:

(i) From the computational point of view, the discrepancy might be ascribed to the finite size of our samples. It should be noted, however, that a simulation performed on 8016-atom samples by Horbach *et al* [39] shows a flattening of the same branch at practically the same energy ($\approx$17 meV) as in the present work, so dramatic size effects are not expected[9].

(ii) It should also be considered that because a phenomenological potential was used we cannot guarantee that the dynamics is correctly reproduced, so the disagreement might after all be simply due to the potential used.

(iii) The experimental density of states is obtained through some approximations, for instance the incoherent approximation and the estimation of the multiphonon contribution for neutron scattering and the shape of $C(E)$ for Raman scattering.

(iv) In the simulations the excess states could be overestimated due to unphysical quenching times currently used in molecular dynamics, as pointed out recently by Angell [40].

Nevertheless the semi-quantitative agreement between experiment and simulation is evident, and suggests the conclusion that the modes responsible for the BP are due to the flattening of the transverse dispersion curve.

This picture is in agreement with the recent theoretical work of Taraskin *et al* [14], who associate the BP with the glassy counterpart of the lowest energy van Hove singularity of the corresponding crystalline structure. In this respect, it is worth noting that the transverse acoustic branch at Q larger than $\approx$8 nm^{-1} is the glassy counterpart of a transverse optic phonon branch of α-quartz (almost flat at $\approx$4 THz, i.e. $\approx$16 meV). This branch, in the extended Brillouin zone scheme which is more appropriate for disordered materials, is the extension of the transverse acoustic branch [41]. According to Boysen *et al* [42], close to the M point of the α-quartz Brillouin zone this branch is strongly temperature dependent, and its softening is responsible for the α–β transition in quartz. More importantly, the atomic displacements induced by the lattice modes of this branch in quartz, as determined in [41], are very similar to the frustrated rotations of SiO_4 tetrahedra which—according to Buchenau *et al* [5]—are in vitreous silica the modes contributing to the BP. All this evidence speaks in favour of a transverse branch origin of the boson peak.

[9] In [39], the BP energy is determined by the maximum of the hump observed in the *dynamical structure factor*, which is a different definition to the one adopted here, i.e. the maximum of the excess density of states. Indeed, the dynamics structure factor (actually its high Q limit) compares directly with the density of states divided by ω^2, while the density of states itself compares directly with the high Q limit of the current spectrum.

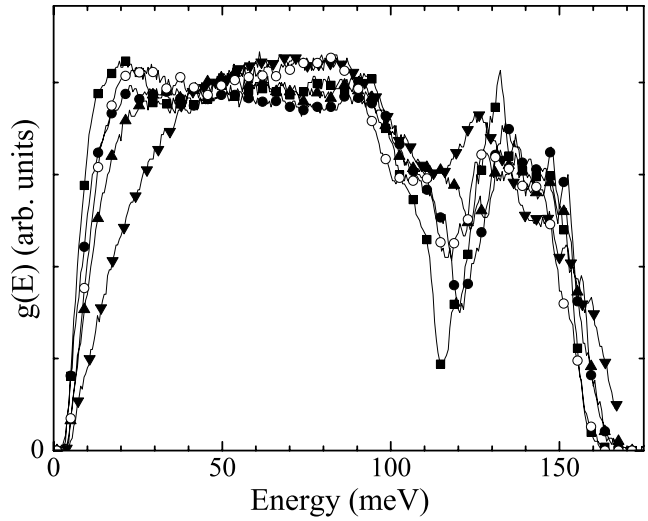

Figure 6. The vibrational density of states of v-SiO_2 at different densities: full squares: $\rho = 2.2$ g cm^{-3}; full circles: $\rho = 2.8$ g cm^{-3}; upward pointing triangles: $\rho = 3.2$ g cm^{-3}; downward pointing triangles: $\rho = 4.0$ g cm^{-3}; open circles: compressed sample $\rho = 2.8$ g cm^{-3} (zero pressure after pressure cycle).

The present MD simulation work adds a further element in support of this point of view. Indeed, the most stringent evidence as to the assignment of the BP to the flattening of the transverse acoustic branch is provided by the behaviour of the high energy transverse dynamics upon densification. Experimentally, it is observed that upon densification (i) the BP energy shifts to higher energy and (ii) its intensity strongly decreases [24, 43, 44]. From our simulations (see figures 4 and 7 for a more complete set of data), we observe that, on increasing the density, the T branch for moderate density flattens at a higher energy with respect to the room pressure sample, and then, upon further densification, no flattening is observed at all. This behaviour parallels that of the calculated density of states as a function of the density, reported for selected mass densities in figure 6. The low energy part of the total density of states shifts towards higher frequencies and decreases in intensity with increasing mass density. As a consequence, the BP strongly decreases in intensity and shifts to high energies [27].

In figure 7 we present the maxima of the transverse currents computed at several densities. For the $\rho = 2.2$ g cm^{-3} sample, after a linear increase, a flattening of the transverse currents is observed for Q values higher than 6 nm^{-1}, at about 15–20 meV. This plateau progressively shifts to higher energy, and eventually disappears with increasing density. For the highest density sample it is no longer observed and only a linear dispersion relationship is present. These latter observations, which are in excellent qualitative agreement with the experimental findings [24, 43, 44], give decisive support to the assignment of the BP to the flattening of the quasi-TA branch.

4. Conclusions

In conclusion, by studying the density dependence of the spectra of the transverse currents, and by comparing them with the experimental mass density dependence of the boson peak in vitreous silica, we propose that the BP itself could be due to quasi-transverse acoustic modes, whose dispersion relation becomes Q independent at high Q, thereby giving rise to

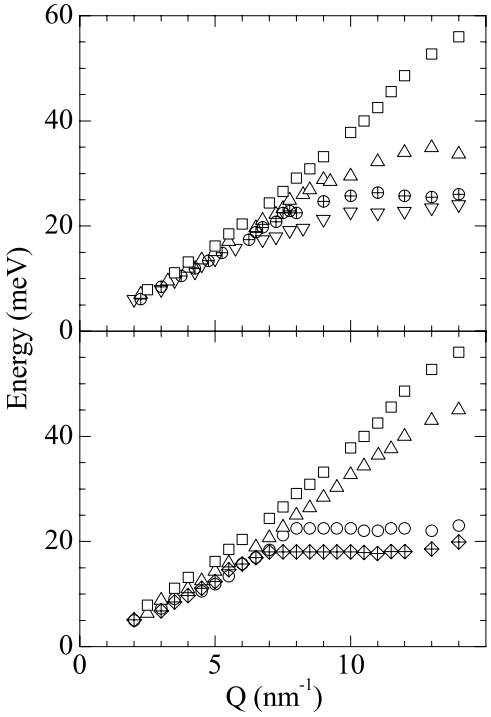

Figure 7. Lower panel: the maximum of the transverse current spectra computed at different densities with increasing density. Diamonds, circles, triangles, and squares correspond to $\rho = 2.2$, 2.8, 3.2, and 4.0 g cm^{-3}, respectively. Upper panel: the maximum of the transverse current spectra measured at different densities with decreasing density. Downward pointing triangles, circles, upward pointing triangles, and squares correspond to $\rho = 2.4$, 2.8, 3.2, and 4.0 g cm^{-3}, respectively. The crossed symbols refer to the zero-pressure realization, before and after the pressure cycle.

an excess of modes with respect to the Debye behaviour. The whole picture presented here reconciles different previous studies on the origin of the BP and yields a fully consistent scenario: (i) the high Q part of the transverse acoustic branch in vitreous silica—which gives rise to the BP—is the counterpart of a low lying transverse optical branch for α-quartz [41]; (ii) according to Boysen *et al* [42] the softening of this branch at the M point produces the α-to-β transition; (iii) in agreement with (i) and (ii), and according to Taraskin *et al* [14, 17], the BP arises from the softening of the lowest energy van Hove singularity of the corresponding crystals; (iv) according to Dorner and co-workers [41] the eigenvectors of this branch for quartz correspond to rotations of SiO_4 tetrahedra; (v) finally, in agreement with (i) and (iv), according to Buchenau *et al* [5] the modes contributing to the BP are hindered rotations of SiO_4 tetrahedra.

Acknowledgments

This work was supported by INFM Iniziativa di Calcolo Parallelo, and by MURST Progetto di Ricerca di Interesse Nazionale. One of us (GR) acknowledges illuminating discussions with U Buchenau and B Dorner.

References

[1] Phillips W A 1981 *Amorphous Solids: Low-Temperature Properties* (Berlin: Springer)
[2] Fontana A and Viliani G 2002 *8th Int. Workshop on Disordered Systems (Andalo, Italy)*; *Phil. Mag.* **82** (special issue)
[3] Anderson P W, Halperin B I and Varma C J 1972 *Phil. Mag.* **25** 1
[4] Phillips W A 1972 *J. Low Temp. Phys.* **7** 351
[5] Buchenau U *et al* 1986 *Phys. Rev.* B **34** 5665
[6] Benassi P *et al* 1996 *Phys. Rev. Lett.* **77** 3835
Benassi P *et al* 1997 *Phys. Rev. Lett.* **78** 4760
Masciovecchio C *et al* 1997 *Phys. Rev.* B **55** 8049
[7] Foret M *et al* 1996 *Phys. Rev. Lett.* **77** 3831
Foret M *et al* 1997 *Phys. Rev. Lett.* **78** 4669
[8] Taraskin S N and Elliott S R 1997 *Phys. Rev.* B **56** 8605
[9] Dell'Anna R, Ruocco G, Sampoli M and Viliani G 1998 *Phys. Rev. Lett.* **80** 1236
[10] Schirmacher W, Diezemann G and Ganter C 1998 *Phys. Rev. Lett.* **81** 136
[11] Surovtsev N V, Wiedersick J, Novikov V N, Rössler E and Duval E 1999 *Phys. Rev. Lett.* **82** 4466
[12] Fontana A *et al* 1999 *Europhys. Lett.* **47** 56
[13] Pilla O *et al* 2000 *Phys. Rev. Lett.* **85** 2136
[14] Taraskin S N, Loh Y L, Natarajan G and Elliott S R 2001 *Phys. Rev. Lett.* **86** 1255
[15] Feldman J L, Allen P B and Bickham S R 1999 *Phys. Rev.* B **59** 3551
[16] Taraskin S N and Elliott S R 1998 *Phil. Mag.* B **72** 403
[17] Taraskin S N, Ludlam J J, Natarajan G and Elliott S R 2002 *Phil. Mag.* B **82** 197
[18] Grigera T S, Martín-Mayor V, Parisi G and Verrocchio P 2001 *Phys. Rev. Lett.* **87** 085502
[19] Götze W and Mayr M R 2000 *Phys. Rev.* E **61** 587
[20] Theenhaus T, Schilling R, Latz A and Letz M 2001 *Preprint* cond-mat 0105393
[21] Zha R A, Hemley R J, Mao H K, Duffy T S and Meade C 1994 *Phys. Rev.* B **50** 13105
[22] Sugai S and Onera A 1996 *Phys. Rev. Lett.* **20** 4210
[23] Inamura Y, Arai M, Yamamuro O, Inaba A, Kitamura N, Otomo T, Matsuo T, Bennington S M and Hanon A C 1999 *Physica* B **263/264** 299
[24] Inamura Y *et al* 2000 *Physica* B **284–288** 299
[25] Lacks A C 2000 *Phys. Rev. Lett.* **84** 4629
[26] Jund P and Jullien R 2000 *J. Chem. Phys.* **113** 2768
[27] Pilla O, Angelani L, Fontana A, Gonçalves J R and Ruocco G 2003 *J. Phys.: Condens. Matter* **S995** 15
[28] Foret M, Vacher R, Courtens E and Monaco G 2002 *Phys. Rev.* B **66** 024204
[29] Foret M, Courtens E, Helen B, Rufflé B and Vacher R 2002 *Phys. Rev.* B **66** 024204
[30] Rufflé B, Foret M, Courtens E, Vacher R and Monaco G 2003 *J. Phys.: Condens. Matter* **15** 1281
[31] van Beest B W H, Kramer G J and van Santen R A 1990 *Phys. Rev. Lett.* **64** 1955
[32] Horbach J, Kob W and Binder K 2001 *Eur. Phys. J.* B **19** 531
[33] Ruocco G and Sette F 2001 *J. Phys.: Condens. Matter* **13** 9141
[34] Leadbetter A J 1969 *J. Chem. Phys.* **51** 779
[35] Sampoli M, Ruocco G and Sette F 1997 *Phys. Rev. Lett.* **79** 1678
[36] Sette F, Ruocco G, Krisch M, Masciovecchio C, Verbeni R and Bergmann U 1996 *Phys. Rev. Lett.* **77** 83
Ruocco G and Sette F 1999 *J. Phys.: Condens. Matter* **11** R259
[37] Carini G, D'Angelo G, Tripodo G, Fontana A, Leonardi A, Saunders G A and Brodin A 1995 *Phys. Rev.* B **52** 9342
[38] Fontana A, Rossi F, Carini G, D'Angelo G, Tripodo G and Bartolotta A 1997 *Phys. Rev. Lett.* **78** 1078
[39] Horbach J, Kob W and Binder K 1998 *J. Non-Cryst. Solids* **320** 235
[40] Angell C A, Yue Y, Wang L-M, Copley J R D, Borik S and Mossa S 2003 *J. Phys.: Condens. Matter* **15** S1051
[41] Strauch D and Dorner B 1993 *J. Phys.: Condens. Matter* **5** 6149
Schober H, Strauch D, Nutzel K and Dorner B 1993 *J. Phys.: Condens. Matter* **5** 6155
[42] Boysen H, Dorner B, Frey F and Grimm H 1980 *J. Phys. C: Solid State Phys.* **13** 6127
[43] Inamura Y, Arai M, Otomo T, Kitamura N and Buchenau U 2000 *Physica* B **284–288** 1157
[44] Jund P and Jullien R 2000 *J. Chem. Phys.* **113** 2768